

Comprehensive understanding of size-, shape-, and composition-dependent polarizabilities of Si_mC_n ($m, n = 1-4$) clusters

You-Zhao Lan, Hong-Lan Kang, Tao Niu

Institute of Physical Chemistry, Zhejiang Normal University, Jinhua 321004, China

Correspondence to: You-Zhao Lan (E-mail: lyzhao@zjnu.cn)

Abstract

We performed a comprehensive study of the size-, shape-, and composition-dependent polarizabilities of Si_mC_n ($m, n = 1-4$) clusters on the basis of the density-functional-based coupled perturbed Hartree-Fock calculations. We found better correlations between the polarizabilities and both the binding energies (E_b) and change in charge distribution (Δq) than the energy gaps (E_g). The α values exhibit overall decreasing and increasing trends with increases in the E_b and Δq values, respectively. For isomers with the same E_b values and different polarizabilities, Δq can well explain the difference in polarizabilities. The π -electron delocalization effect is the best factor for understanding the shape-dependence. For a given m/n value, the linear clusters have an obviously larger polarizability than both the prolate and compact clusters, irrespective of the cluster size. We fit a quantitative expression [$\alpha = A - (A - B) \times \exp(-k(m/n))$] to describe the composition-dependent polarizabilities.

Keywords: Binding energy, energy gap, charge distribution, polarizability, silicon carbide cluster

1. Introduction

In the last 20 years, the (hyper)polarizabilities of small semiconductor clusters such as gallium arsenide (GaAs), silicon (Si), silicon carbide (SiC), and aluminum phosphide (AlP) clusters have attracted much attention [1-27]. Experimental studies have shown that the static polarizabilities of Si_m ($m = 9-50$) and Ga_mAs_n ($m + n = 5-30$) clusters fluctuate around their corresponding bulk values [12]. These experimental results have motivated many theoretical studies of the polarizabilities of Si and GaAs clusters [1, 2, 4, 6 - 9, 16, 26, 27]. Theoretical studies have shown that the size of the polarizability directly or indirectly depends on various factors such as the cluster size, cluster shape, cluster composition, energy gap, binding energy, ionization potential, and so on. The size-dependence of the polarizabilities has been well known for Si and GaAs clusters. For small Si_m ($m < 10$) and Ga_nAs_m ($n + m < 8$) clusters, the theoretical polarizabilities are higher than the bulk value and decrease with an increase in cluster size [1, 2, 9, 12, 16], as indicated by the number of atoms in a cluster. For mediate-size Si_m ($m = 9-50$) and

Ga_nAs_m ($n + m = 5\text{--}30$) clusters, the experimental polarizabilities [12] vary strongly and irregularly with the cluster size and fluctuate around the bulk value. For large Si_m ($m = 60\text{--}120$) clusters, all the experimental polarizabilities are lower than the bulk value [12]. However, for Si_m ($m = 9\text{--}28$) clusters, Deng *et al.* [6] found that the theoretical polarizabilities exhibit fairly irregular variations with the cluster size, and all the calculated values are higher than the bulk value. Similar theoretical results have also been obtained by Sieck *et al.* [21] and Jackson *et al.* [7] for Si_m ($m = 1, 3\text{--}14, 20, \text{ and } 21$) and ($m = 1\text{--}21$) clusters, respectively. Until now, the discrepancies between the experimental and theoretical polarizabilities have not been well explained [6,7]. More investigation is required.

The shape-dependence of the polarizabilities has also been known for Si, GaAs, and AIP clusters [4, 7, 23, 28]. For Si_m ($m = 20\text{--}28$) clusters, the prolate clusters have a systematically larger polarizability than the compact ones [4]. This shape-dependence reflects the metallic character of these Si_m ($m = 20\text{--}28$) clusters, because it is reproduced by using the jellium models. For the prolate $(\text{GaAs})_n$ and $(\text{AIP})_n$ clusters [22, 23, 28], the (hyper)polarizabilities monotonically increase with an increase in n . This trend is very similar to the well known (hyper)polarizability evolution of extended conjugated organic molecules [29]. We also notice other interesting shape-dependences of the polarizabilities. For $\text{Co}_n(\text{C}_6\text{H}_6)_m$ ($n, m = 1\text{--}4, m = n, n + 1$) clusters [30], the sandwich clusters have systematically larger polarizabilities and anisotropies than the rice-ball isomers, which suggests that we should distinguish these two kinds of clusters in terms of their dipole polarizabilities. The (hyper)polarizabilities of the Möbius, normal cyclacene, and linear nitrogen-substituted strip polyacenes exhibit clear shape-dependence [31]. The shape-dependence based on the geometries of the cyclacene with and without a knot, namely, Möbius and normal cyclacene, is very different from that based on the linear, prolate, and compact geometries of semiconductor clusters. Therefore, more different shape-dependences could be considered for semiconductor clusters in the future. The composition-dependence of the polarizabilities is only available for heteratomic clusters and is less known than the size- and shape-dependences for semiconductor clusters [12, 26]. Karamanis *et al.* [26] investigated the composition-dependent polarizabilities of open- and closed-shell Ga_mAs_n clusters with $m + n = 5$ and 6. They showed that for a given size (5 or 6), the polarizabilities of the Ga_mAs_n clusters gradually increase with an increase in the number of Ga atoms in a cluster. This dependence implies that for the heteratomic clusters, we can obtain a tunable polarizability by adjusting the composition of the clusters.

Understanding the evolution of the polarizability is essential for nanomaterial design. For example, on the basis of the composition-dependence of the polarizability, we have more choices to obtain different polarizabilities by adjusting cluster composition. Although the size-dependence has generally been correlated with the energy gaps (E_g) between the highest occupied molecular orbital (HOMO) and lowest unoccupied molecular orbital (LUMO), many studies have shown that the correlation between α and E_g is very poor [4, 6–8]. Therefore, it is necessary and interesting to seek other factors to understand the size-dependent polarizabilities. In this work, we find better correlations between the polarizabilities and binding energies (E_b) than E_g . For the isomers with the same E_b values and different α values, we show that the change in the charge distribution (Δq) can be used to understand the size of the polarizability. Meanwhile, to explicitly describe the composition-dependent polarizabilities, we fit a quantitative expression for the relationship between the α values and the cluster composition such as m/n in the Si_mC_n clusters.

In Section 2, we provide the computational details. In Section 3, we discuss the size-, shape-,

and composition-dependent polarizabilities of Si_mC_n ($m, n = 1-4$) clusters. Finally, we summarize our results in Section 4.

2. Computational Details

There have been many studies on the geometry and electronic structure of small SiC clusters. Low-lying isomers of these clusters have been theoretically or experimentally determined. For the purpose of our present work, we selected the lowest-lying isomers and some low-lying isomers with different shapes (*i.e.*, linear (chain), prolate (flat), and compact clusters) of the Si_mC_n ($m, n = 1-4$) clusters on the basis of the literature [32–35]. Note that for the small clusters considered here, the linear and prolate isomers have linear chain and flat forms, respectively, which is different from the classification for the larger clusters reported in previous studies. Although a linear geometry can be considered to be prolate, for the small clusters of less than ten atoms considered in this work, linear clusters have obviously different polarizabilities from the prolate clusters. Therefore, these linear clusters were classified individually. For a given shape, the selected low-lying isomers had the lowest energy. For example, the linear $D_{\infty h}$ structure was the lowest-lying isomer or ground-state structure of Si_2C_3 , whereas the C_{2v} prolate structure was the lowest energy isomer for the prolate Si_2C_3 clusters [32]. Note that there have been some discrepancies between the results of theoretical and experimental studies on the ground-state structure of SiC clusters (even small clusters). For instance, most theoretical and experimental studies [36–39] have revealed that SiC_3 has three stable isomers (two having four-membered rings (C_{2v} , 1A_1) and one with a linear structure ($C_{\infty v}$, $^3\Sigma$)) and that the global minimum structure of SiC_3 is a C_{2v} prolate with a transannular C–C bond. However, these results are still controversial because the linear structure was predicted to be the ground state structure on the basis of highly accurate coupled cluster methods, including a perturbative treatment of triple excitations and Dunning’s correlation-consistent polarized core-valence quadrupole zeta basis set [CCSD(T)/cc-pCVQZ] [40]. In the Si_2C cluster [32, 33], the C_{2v} and $D_{\infty h}$ singlet structures compete for the ground-state structure, depending on the level of theory. All of the selected clusters were re-optimized at the DFT/aug-cc-pVTZ level using the hybrid Becke3-Lee-Yang-Parr (B3LYP) functional. The vibrational frequencies were calculated to confirm that the final geometries are stable without an imaginary frequency. The final geometries and their electronic states, symmetries, cluster shape, binding energies (E_b), and energy gaps (E_g) are shown in figure 1.

For the estimation of the dipole polarizability (α), we focused on the isotropic dipole polarizability ($\langle\alpha\rangle$), which is defined as $\langle\alpha\rangle = 1/3(\alpha_{xx} + \alpha_{yy} + \alpha_{zz})$. The $\langle\alpha\rangle$ is expressed in $\text{\AA}^3/\text{atom}$. Hereafter, α refers to $\langle\alpha\rangle$. To obtain accurate dipole polarizabilities, we should select an appropriate theoretical method and reasonable basis set. In general, the diffuse and polarization functions and electron correlation effects should be considered in the calculation. For density-functional-based methods, the local density approximation (LDA) and general gradient approximation (GGA) functionals can produce the close dipole polarizabilities. For example, the Vosko-Wilk-Nusair (VWN), BLYP, and B3LYP functionals produce polarizabilities of 5.17, 5.52, and 5.37 $\text{\AA}^3/\text{atom}$ for the C_{2v} singlet Si_3 cluster [8], respectively. Different hybrid functionals such as the B3LYP, B3P86, and B3PW91 functionals also produce very close polarizabilities [16, 22]. For wave-function-based methods, the Møller-Plesset second order perturbation theory (MP2) with the aug-cc-pVDZ or 6-31G augmented by the standard diffuse and polarization functions can

lead to accurate dipole polarizabilities, which are very close to the results based on highly accurate coupled cluster singles-and-doubles calculations, including a perturbative triples correction for binary semiconductor clusters such as AIP and GaAs clusters [22–24, 26]. A more detailed discussion of the basis-set and theoretical method dependences of α for small Si and SiC clusters can be found elsewhere [2, 8, 9, 15, 16]. In this work, we calculated the polarizabilities by using the coupled perturbed Hartree–Fock (CPHF) approach at the B3LYP/aug-cc-pVTZ level. A test B3LYP/aug-cc-pVTZ calculation performed on a CO molecule gave a polarizability of 1.95 \AA^3 , which is in good agreement with the experimental [41] and theoretical [42] value of 1.95 \AA^3 . The calculated polarizabilities are also shown in figure 1. The polarizability of the SiC molecule was calculated using both the CPHF and finite field (FF) method at the aug-cc-pVTZ level to make a comparison with previous results [43] and because there was no appropriate symmetry (α_{xx} : 57.35, α_{yy} : 34.46, and α_{zz} : 59.54 a.u.) of the three polarizability components based on the CPHF/B3LYP calculation. The FF/B3LYP and FF/MP2 methods based on the fields of 0.003 (parallel) and 0.001 (perpendicular) a.u. give isotropic polarizabilities of 4.40 and $3.84 \text{ \AA}^3/\text{atom}$, respectively. The FF/MP2/aug-cc-pVTZ result is in agreement with the polarizability of $3.86 \text{ \AA}^3/\text{atom}$ based on the FF/MP2 with a self-designed basis set [43] and the fields of 0.003 (parallel) and 0.001 (perpendicular) a.u. The FF/B3LYP/aug-cc-pVTZ result was used for the SiC molecule in the following discussion. All of the calculations were performed using the Gaussian 03 program [44].

3. Results and Discussion

3.1. Size-dependence

We first investigate the size-dependent polarizabilities of Si_mC_n ($m, n = 1-4$) clusters. It can be expected that the size-dependence of polarizabilities of heteroatomic clusters will be more complicated than that of homoatomic clusters because heteroatomic clusters with a given cluster size have more isomers than homoatomic ones. Figure 2 shows the size-dependent polarizabilities of Si_mC_n ($m, n = 1-4$) clusters. The cluster size is indicated by the number of atoms (N) in cluster. For comparison, the polarizabilities based on the B3LYP calculations of Si_m ($m = 1-8$) (Ref. [8, 16]), and C_n (linear: $n = 1-8$; cyclic: $n = 4, 6$, and 8) (Ref. [45]) clusters are included in figure 2. In Ref. [45], the α values of the C_n ($n = 1-8$) clusters were calculated using a self-designed basis set that is different from the aug-cc-pVTZ we used here. Therefore, we recalculated the α values of C_n ($n = 1-8$) clusters to check the difference caused by the basis set effect. The obtained results are close to those of Ref. [45] and the difference is lower than $\sim 0.03 \text{ \AA}^3/\text{atom}$. For example, we obtained a polarizability of 1.86 \AA^3 for C atom, which is close to 1.88 \AA^3 reported in Ref. [45]. The Si, SiC, and C bulk values are also included in figure 2 and they are 3.71 (Ref. [1]), 1.84 (Ref. [15]), and $0.83 \text{ \AA}^3/\text{atom}$, respectively, which were obtained according to the Clausius-Mossotti relation. We calculated the C bulk value on the basis of the dielectric constant of 5.7 and the diamond density of 3.51 g/cm^3 . As expected, small SiC clusters have a more complicated size-dependence of α than small Si and C clusters. For small Si_m ($m < 10$) clusters, the α values are higher than the corresponding bulk value and decrease with an increase in cluster size [1, 8, 12, 16, 45]. For small linear C_n ($n \leq 8, n \neq 2$) clusters, we can observe an increasing trend with an increase in cluster size, which is attributed to an increasing trend of longitudinal component of α . For small SiC clusters, we cannot observe a simple trend as small Si and C clusters. As shown in figure 2, the α values of Si_mC_n ($m, n = 1-4$) clusters are higher than the corresponding bulk value and have an oscillating variation with the cluster size.

We can also see from figure 2 that the α values of the SiC clusters lie between those of pure Si and C clusters (*i.e.*, an order of $\alpha(\text{Si}) > \alpha(\text{SiC}) > \alpha(\text{C})$), especially when the cluster size is fixed. For example, for diatomic clusters, Si_2 , SiC, and C_2 clusters, their polarizabilities are 7.35, 4.30, and $3.63 \text{ \AA}^3/\text{atom}$, respectively. The same case occurs for triatomic clusters. For some given cluster sizes, this order does not hold and the SiC cluster has a larger α than the Si cluster or a smaller α than the C cluster. For example, for $n = 6$, the linear Si_2C_4 cluster has a larger α of $5.07 \text{ \AA}^3/\text{atom}$ (figure 1) than the compact Si_6 cluster with $4.56 \text{ \AA}^3/\text{atom}$. For $n = 8$, the linear C_8 cluster has a larger α of $3.13 \text{ \AA}^3/\text{atom}$ than the prolate $\text{C}_s(\text{b}) \text{Si}_4\text{C}_4$ cluster with $2.94 \text{ \AA}^3/\text{atom}$ (figure 1). These exceptions exist because for these clusters the shape effect (*i.e.*, linear π delocalized structure) significantly determines the size of α (see discussion below). For $N > 10$, a comparison can not be made because of lack of the polarizabilities of the SiC clusters.

To understand the size of α of the clusters, we first consider the approach based on the energy gap. In the sum-over-states (SOS) expression of polarizability obtained from the simple perturbation theory,

$$\alpha_{ii} = 2 \sum_{k,l} \frac{|\langle k | \mu_i | l \rangle|^2}{E_l - E_k},$$

where the matrix element $\langle k | \mu_i | l \rangle$ corresponds to the transition dipole moment between occupied (l) and unoccupied (k) states in the i th direction, and $E_l - E_k$ is the corresponding transition energy, if we assume that the transitions between the HOMO and the LUMO make a major contribution to the polarizability, then the α can be inversely related to the E_g (Refs. [1, 7, 8]). However, the inverse relationship between α and E_g does not hold in general. For Si_m ($m < 30$) clusters, theoretical researches have shown that the correlation between α and E_g is very weak [4, 6, 7]. For example, for Si_m ($m = 11-28$) clusters, the overall distribution in the plot of α versus E_g is very scattered [6]. However, a research on the germanium clusters with 2 – 25 atoms [46] have shown a well correlation between α and E_g , that is, the size of α is inversely related to the size of E_g and a molecule with a smaller E_g is found to be softer and has a larger α . To understand the lack of correlation between E_g and α , Pouchan *et al.* [8] have shown that this lack can be understood as the vanishing matrix element $|\langle k | \mu_i | l \rangle|^2$ between HOMO and LUMO in the SOS expression for some clusters, especially for the cluster with small size and high symmetry, and they have made a direct correlation between the α and the lowest symmetry-allowed transition energy gap not the energy gap for small Si_m ($m = 3-10$) clusters on the basis of the density function calculations with different functionals. In figure 3, we plot the α values versus the E_g values (figure 1) for Si_mC_n ($m, n = 1-4$) clusters. The results reveal an irregular correlation between α and E_g and a very scattered overall distribution.

On the other hand, one correlates the size of α with E_g on the basis of the inverse relationship between α and hardness. A harder molecule [47] has a larger E_g , in other words, a stable system with a large E_g (Ref. [48]) has a low polarizability according to the minimum polarizability principle [49–51] which points out that “the natural direction of evolution of any system is towards a state of minimum polarizability”. Note that the stability of a system can be also related to its E_b value [48], that is, a stable system has a large E_b . Therefore, we secondly attempt to correlate α with E_b . Figure 4 shows the plots of α versus E_b for Si_mC_n ($m, n = 1-4$) clusters. Compared with E_g , the α values have an overall decreasing trend with an increase of the E_b values, which is approximately indicated by a dot line in figure 4. In the following discussions, we will

find a better correlation between α and E_b when both the cluster shape and one of the components in cluster are fixed.

Thirdly, we correlate the size of α with the change in charge distribution related to an external field. Jackson *et al.* [4] used this approach to reveal that the response of the compact and prolate Si_m ($m = 20 - 28$) clusters to a static external field is metallic on the basis of the metallic-like distribution of charge in these clusters. Karamanis *et al.* [22] employed this approach to show that the bonding effect is more important than the cluster composition on the hyperpolarizability values for a series of Al_nP_n ($n = 2, 3, 4, 6, \text{ and } 9$) clusters. The response of a molecule to an external field leads to a redistribution of atomic charge in cluster, especially for the surface atoms [4]. In our present work, we used a modified parameter:

$$\Delta q = \frac{1}{3N} \sum_j \Delta q_j = \frac{1}{3N} \sum_j \sum_i^N |q_i(F_j) - q_i(0)|$$

to characterize the redistribution of charge, where N is the cluster size, $q_i(F_j)$ is the natural charge of atom i perturbed by a F_j external field in the direction $j = x, y, z$, and $q_i(0)$ is the natural charge of an unperturbed molecule. To obtain distinct Δq values, we applied a strong field of 0.02 a.u. to calculate the natural charge. We collected the calculated results in table 1 where three polarizability components (α_{xx} , α_{yy} , and α_{zz}) are also included. From table 1, we observe the same size order for the components of α and Δq . For example, the prolate SiC_2 cluster has orders of $\alpha_{xx} < \alpha_{yy} < \alpha_{zz}$ and $\Delta q_x < \Delta q_y < \Delta q_z$. We assume that the cluster with a larger Δq would have a larger polarizability because the electric polarization leads the charge distribution of a molecule to distort from its normal shape. Figure 5 shows the plots of α versus Δq for the Si_mC_n ($m, n = 1 - 4$) clusters. Compared with the E_g , the α values have an overall increasing trend with an increase of the Δq values, which is approximately indicated by a dot line in figure 5. Similar to the E_b , we will find a better correlation between α and Δq provided that both the cluster shape and one of the components in cluster are fixed (see discussion below).

3.2. Shape-dependence

It is well known that organic molecules with a linear or prolate geometry have a large (hyper)polarizability because they have a delocalized π -conjugated structure [29, 52]. Constructing a π -conjugated structure has become one of choices to design a new molecule with large (hyper)polarizability [53]. For small SiC clusters with increasing the cluster size, three alternative hybridizations (sp , sp^2 , and sp^3) of C atom result in a variation from linear to prolate, then compact structure in lowest-lying isomers while the sp^3 hybridization of Si atom leads to a variation from prolate to compact structure. A transition from prolate to compact will lead to a decrease of the electron delocalization, ultimately, a decrease of the (hyper)polarizability [22, 24]. Experimental and theoretical studies have provided sufficient information on the geometry [32, 33, 54–59] for Si_mC_n ($n + m < 8$) clusters. The structure of the SiC cluster is a result of the competition for bonding that occurs between the C and Si atoms. As shown in figure 1, C-rich clusters tend to exist in the linear or prolate structure while Si-rich clusters prefer forming prolate or compact structure. For example, the lowest-lying isomers of SiC_n ($n = 2, 3, \text{ and } 4$) clusters are the linear structure while those of Si_mC ($m = 2, 3, \text{ and } 4$) clusters are prolate or compact structure (figure 1). In our recent work [15], we have shown that the size-dependence of the first-order hyperpolarizabilities of SiC_n ($n = 2 - 6$) clusters, which have approximate Si-terminated linear chain geometry, is similar to that observed in π -conjugated organic molecules. For semiconductor

clusters such as Si, AlP, and GaAs clusters, theoretical researches have shown that the prolate clusters have systematically larger polarizabilities than the compact ones [4, 6, 7, 22, 23, 27, 28]. Therefore, the size of the (hyper)polarizability, to some degree, depends on the geometry or shape of a cluster.

Figure 6 shows the shape-dependence of α for Si_mC_n ($m, n = 1-4$) clusters. Although no clear correlation is observed between the size of α and the cluster shape from figure 6, we can see that most of the linear clusters have a large α and the shape-dependence of α will be clear when the cluster size and composition are fixed. For example, for triatomic clusters (Si_2C and SiC_2), the linear and prolate Si_2C clusters have the α values of 4.18 and 4.03 $\text{\AA}^3/\text{atom}$, respectively, and for the linear and prolate SiC_2 clusters they are 2.73 and 2.25 $\text{\AA}^3/\text{atom}$, respectively (figure 1). A similar case occurs for tetra-atomic clusters (Si_2C_2 and SiC_3 clusters). In detail, figure 7a shows the plots of the α values versus the number of C atoms (n) in cluster with both the cluster shape and the number of Si atoms fixed. From figure 7a, we can clearly observe orders of $\alpha(\text{L}) > \alpha(\text{P})$ and $\alpha(\text{P}) > \alpha(\text{C})$ for a given composition. For the prolate and compact series clusters, the α values decrease with an increase of the number of C atoms (n) in cluster, which indicates a composition-dependence of α (see discussion below).

To understand the shape-dependence of α for the Si_mC_n ($m, n = 1 - 4$) clusters, we attempt to use the following approaches:

(1) Using both E_g and E_b . As mentioned above, both E_g and E_b have no regular overall variation with the size of α . In figures 7b and 7c, we plot the E_b and the E_g versus the number of C atoms (n) in cluster, respectively, corresponding to the clusters considered in figure 7a. On the basis of the SOS expression, we would have a larger α for the cluster with a smaller E_g , but in figure 7c this behavior has not been observed for all clusters except SiC_4 (L and P) and Si_3C_3 (P and C). Therefore, the shape dependence cannot be explained by the E_g even when both the cluster size and the cluster shape are fixed, in accord with the Jackson *et al.* [4] who had shown that the differences between the α values of the prolate and compact clusters cannot be explained on the basis of the E_g for Si_m ($m = 20-28$) clusters. For the E_b , for all series of clusters except Si_2C_n (L) we can observe an inverse relationship between α and E_b , in agreement with the fact that a cluster has a high stability and a low polarizability.

(2) Using a geometrical parameter,

$$I = \sum_{i=1}^n r_i^2,$$

where r_i is the distance of atom i to the cluster center of mass and n is the number of atoms in cluster. Deng *et al.* [6] used this approach to explain the evolution of α for Si_m ($m = 9 - 28$) clusters and showed that more elongated clusters are more polarizable. However, Jackson *et al.* [4] found that the shape-dependence of the *total* polarizabilities is clearly more complicated than the difference in I between the compact and prolate Si_m ($m = 20-28$) clusters. For the SiC clusters we considered here, the I values are close between different shape clusters especially for a given cluster size because the clusters have small size ($N \leq 8$). Therefore, this approach is not available for the systems considered here.

(3) Using the Δq defined above. In figure 7d, we plot the Δq versus the number of C atoms (n), corresponding to the clusters considered in figure 7a. Combining with figure 7a, we can see that the shape dependence of α cannot be reflected by the size of the Δq . For example, for the linear and prolate Si_2C_n clusters with a given n , the linear Si_2C_n cluster has a larger α than compact Si_2C_n

one (figure 7a) while the size orders of Δq between prolate and compact clusters alternately change with increasing the number of C atoms (n) (figure 7d). For the prolate and compact Si_3C_n clusters with a given n , reverse size orders are observed for the α and Δq values. However, it is interesting that the α values have the same variation trend as the Δq with an increase of the number of C atoms for each series of clusters. Comparing figure 7d with figure 7b, we can see that the Δq is more available than the E_b for qualitatively understanding the size of α . For instance, for both the linear and the prolate Si_2C_n clusters, the Δq values can well reflect the evolutions of α (figure 7a and figure 7d) while the E_b values cannot (figure 7a and figure 7b). Furthermore, some isomers with very close E_b values and different α values may be identified by the Δq values. For example, for $\text{Si}_4\text{C}_4(\text{C}_{2v})$, $\text{Si}_4\text{C}_4(\text{C}_s(\text{a}))$, and $\text{Si}_4\text{C}_4(\text{C}_s(\text{b}))$ clusters whose E_b values are 4.486, 4.484, and 4.487 eV/atom (figure 1), respectively, the size of α ($\text{Si}_4\text{C}_4(\text{C}_{2v})$: 3.46 $\text{\AA}^3/\text{atom}$, $\text{Si}_4\text{C}_4(\text{C}_s(\text{a}))$: 3.36 $\text{\AA}^3/\text{atom}$, $\text{Si}_4\text{C}_4(\text{C}_s(\text{b}))$: 2.94 $\text{\AA}^3/\text{atom}$) is well related to that of Δq ($\text{Si}_4\text{C}_4(\text{C}_{2v})$: 0.125 e/atom, $\text{Si}_4\text{C}_4(\text{C}_s(\text{a}))$: 0.094 e/atom, and $\text{Si}_4\text{C}_4(\text{C}_s(\text{b}))$: 0.076 e/atom, respectively).

(4) Considering the delocalization of π -electron structure. Organic molecules with π -electron delocalization have a large (hyper)polarizability [29, 52] because a π -electron delocalization leads to a strong charge separation. As shown in figure 1, both the linear and the prolate clusters would form a π -electron delocalization framework. Although the transition between the HOMO and the LUMO does not determine the size of α , the transitions between different frontier MOs generally make significant contributions to the size of α on the basis of the SOS expression [15]. To check the distribution of electron, we provide in figure 8 the HOMO-1, HOMO, LUMO, and LUMO+1 of SiC_2 , SiC_4 , Si_3C_2 , Si_3C_3 , and Si_4C_4 clusters based on the B3LYP/aug-cc-pVTZ wave function. It is clearly shown that for a given cluster size, the linear cluster has more π -delocalized frontier molecular orbital (MO) than the prolate one. For example, the linear SiC_2 cluster has four π -delocalized MOs (two-fold degenerate HOMO-1 and LUMO) while the prolate SiC_2 cluster has only one π -delocalized MO (LUMO+1). Similarly, for the prolate and compact clusters, the prolate cluster has more obvious π -delocalized MO than the compact one. Therefore, the shape-dependence of α can be well understood on the basis of the electron delocalization of these frontier MOs.

3.3. Composition-dependence

As mentioned above, for heteroatomic clusters such as AlPs and GaAs clusters, the size of α also strongly depends on the cluster composition [25, 26]. Figure 9 shows the plots of the α values versus the m/n values for Si_mC_n ($m, n = 1-4$) clusters. Regardless of the cluster shape, we cannot observe a clear correlation between α and m/n from figure 9. The linear clusters have an obvious larger polarizability than both the prolate and compact clusters especially for a given m/n value. We notice that four linear clusters with small m/n ratio have a large α . These four clusters are SiC , Si_2C_4 , Si_2C_3 , and Si_2C_2 with 4.30, 5.07, 4.26, and 4.75 $\text{\AA}^3/\text{atom}$, respectively. Combining with the shape-dependence of α , we can conclude that the shape effect makes a main contribution to the size of α for these four clusters because they have very different cluster sizes ($N = 2, 6, 5, \text{ and } 4$, respectively) and small m/n ratios (≤ 1.0). When excluding the linear clusters, we can observe an overall increasing trend of α with an increase of m/n . A nonlinear fit for the α values versus the m/n values of the prolate and compact clusters give an expression of $\alpha = A - (A - B) \times \exp(-k(m/n))$, where $A = 4.3$, $B = 1.5$, and $k = 0.87$. The A and B values locate at the region of the α values of pure Si and C clusters, respectively (figure 2). This expression indicates that the α

values of small SiC clusters would tend towards those of pure Si_m clusters with $n = 0$ and towards those of pure C_n clusters with $m = 0$. This dependence is useful for us to design SiC clusters with tunable α values. Note that the tunable polarizabilities presented here are based on the stable clusters. For unstable or metastable clusters such as transition and excited state clusters, the tunable behavior of polarizabilities is difficult to obtain because the excited state polarizabilities are very different from the ground state ones [60, 61].

Similar to the GaAs cluster [26], we can understand the composition-dependence of α in terms of the atomic polarizabilities of C and Si atoms. On the basis of the B3LYP/aug-cc-pVTZ calculations, we obtained the α values of 1.86 and 6.00 \AA^3 for C and Si atoms, respectively. The α value of Si atom is three times larger than that of C atom. As shown in the polarizabilities of GaAs clusters [26], a replacement of As by Ga in cluster will increase the polarizability because the α of Ga atom is almost twice that of As atom. A same case occurs for the SiC cluster we considered here provided that the cluster shape is fixed. Actually, all the lowest-lying GaAs clusters considered by Karamanis *et al.* [26] have a compact structure except that the Ga_4As with a prolate structure has a largest α among four pentaatomic GaAs clusters. In our present work, for $N = 5$, the compact Si_4C (4.11 $\text{\AA}^3/\text{atom}$), prolate Si_3C_2 (3.85 $\text{\AA}^3/\text{atom}$), and linear Si_2C_3 (4.26 $\text{\AA}^3/\text{atom}$) clusters individually have a larger α than the compact Si_3C_2 (3.42 $\text{\AA}^3/\text{atom}$), prolate Si_2C_3 (3.05 $\text{\AA}^3/\text{atom}$), and linear SiC_4 (3.02 $\text{\AA}^3/\text{atom}$) clusters. Note that the linear Si_2C_3 cluster has a largest α , which further implies that the shape effect makes a main contribution to determining the size of α .

From figure 7a, we have seen that the α values decrease with an increase of the number of C atoms (n) when both the cluster shape and the number of Si atoms in clusters are fixed. Furthermore, in figure 10, we plot the α values versus the number of Si atoms (m) with both the cluster shape and the number of C atoms fixed. All of the clusters considered in figure 10 have a prolate structure. Interestingly, we find that the α values increase with an increase of the number of Si atoms (m). In figure 10, we include the plots of E_b , E_g , and Δq versus m to further check the correlation between α and E_b , E_g , and Δq , respectively. As shown in figure 10, both E_b and Δq are more available than E_g for reflecting the size of α , that is, reverse and positive relationships with α for E_b and Δq , respectively, in agreement with the discussions above. Note that for the correlation between α and both E_b and Δq , we can only give the qualitative correlation for all the clusters considered, that is, the α values exhibit overall decreasing and increasing trends with increases in the E_b and Δq values, respectively. We cannot give the generalized quantitative correlation expression for all the clusters considered.

4. Conclusions

We have theoretically investigated the size-, shape-, and composition-dependence of the polarizabilities for small Si_mC_n ($m, n = 1-4$) clusters. The linear and prolate clusters with a delocalized π -electron framework have systematically larger polarizabilities than the compact ones, which is available for many small semiconductor clusters. For example, the prolate Si_3 (C_{2v}), Si_4 (D_{2h}), Al_2P_2 (D_{2h}), Al_3P_3 (D_{3h}), Ga_2As_2 (D_{2h}), and Ga_4As (C_{2v}) clusters have a large polarizability per atom [1, 2, 8, 16, 24, 26]. Although both E_g and E_b are generally used to characterize the stability of the cluster, E_b is more available than E_g for reflecting the size of polarizability. For the isomers with the same E_b values and different polarizabilities, over the factors studied in this work, the Δq allows us to better explain the size-dependence of polarizabilities. The composition-dependence of α suggests that the α values of heteroatomic (A_mB_n) clusters should

gradually converge to those of pure A_m and B_n clusters with an increase and decrease of the m/n value, respectively. We explicitly show by fitting a quantitative expression that a tunable polarizability can be obtained by adjusting the composition in clusters. Finally, to our knowledge, there has been no experimental polarizability for SiC cluster, therefore, for heteroatomic SiC clusters which simultaneously have these three dependences, our present results are useful references for future experiments on the polarizabilities of these clusters.

Acknowledgement

The authors are grateful for the project supported by Scientific Research Fund of Zhejiang Provincial Education Department [Y201119609] and the calculation support provided by the Foundation of Zhejiang Key Laboratory for Reactive Chemistry on Solid Surfaces.

References

- [1] Vasiliev I.; Ögüt S.; Chelikowsky J. R.; *Phys. Rev. Lett.* **1997**, 78, 4805–4808.
- [2] Bazterra V. E.; Caputo M. C.; Ferraro M. B.; Fuentealba P. *J. Chem. Phys.* **2002**, 117, 11158–11165.
- [3] Maroulis G.; Pouchan C. *J. Phys. B: At. Mol. Opt. Phys.* **2003**, 36, 2011–2017.
- [4] Jackson K. A.; Yang M.; Chaudhuri I.; Frauenheim Th. *Phys. Rev. A* **2005**, 71, 033205.
- [5] Mochizuki Y.; Ågren H. *Chem. Phys. Lett.* **2001**, 336, 451–456.
- [6] Deng K.; Yang J. L.; Chan C. T. *Phys. Rev. A* **2000**, 61, 025201.
- [7] Jackson K.; Pederson M.; Wang C. Z.; Ho K. M. *Phys. Rev. A* **1999**, 59, 3685–3689.
- [8] Pouchan C.; Bégué D.; Zhang D. Y. *J. Chem. Phys.* **2004**, 121, 4628–4634.
- [9] Maroulis G.; Bégué D.; Pouchan C. *J. Chem. Phys.* **2003**, 119, 794–797.
- [10] Maroulis G.; Pouchan C. *Phys. Chem. Chem. Phys.* **2003**, 5, 1992–1995.
- [11] Bégué D.; Pouchan C.; Maroulis G.; Zhang D. Y. *J. Comp. Meth. Sci. Eng.* **2006**, 6, 223–231.
- [12] Schäfer R.; Schlecht S.; Woenckhaus J.; Becker J. A. *Phys. Rev. Lett.* **1996**, 76, 471–474.
- [13] Rantala T. T.; Stockman M. I.; Jelski D. A.; George T. F. *J. Chem. Phys.* **1990**, 93, 7427–7438.
- [14] Lan Y. Z.; Feng Y. L.; Wen Y. H.; Teng B. T. *Chem. Phys. Lett.* **2008**, 461, 118–121.
- [15] Lan Y. Z.; Feng Y. L. *J. Chem. Phys.* **2009**, 131, 054509.
- [16] Lan Y. Z.; Feng Y. L.; Wen Y. H.; Teng B. T. *J. Mol. Struct. (THEOCHEM)* **2008**, 854, 63–69.
- [17] Lan Y. Z.; Cheng W. D.; Wu D. S.; Shen J.; Huang S. P.; Zhang H.; Gong Y. J.; Li F. F. *J. Chem. Phys.* **2006**, 124, 094302.
- [18] Lan Y. Z.; Cheng W. D.; Wu D. S.; Li X. D.; Zhang H.; Gong Y. J. *Chem. Phys. Lett.* **2003**, 372, 645–649.
- [19] Korambath P. P.; Karna S. P. *J. Phys. Chem. A* **2000**, 104, 4801.
- [20] Guillaume M.; Champagne B.; Bégué D.; Pouchan C. *J. Chem. Phys.* **2009**, 130, 134715
- [21] Sieck A.; Porezag D.; Frauenheim Th.; Pederson M. R.; Jackson K. *Phys. Rev. A* **1997**, 56, 4890–4898.
- [22] Karamanis P.; Leszczynski J. *J. Chem. Phys.* **2008**, 128, 154323.
- [23] Karamanis P.; Xenides D.; Leszczynski J. *J. Chem. Phys.* **2008**, 129, 094708.
- [24] Karamanis P.; Xenides D.; Leszczynski J. *Chem. Phys. Lett.* **2008**, 457, 137–142.

- [25] Krishtal A.; Senet P.; Alsenoy C. V. *J. Chem. Phys.* **2010**, 133, 154310.
- [26] Karamanis P.; Carbonnière P.; Pouchan C. *Phys. Rev. A* **2009**, 80, 053201.
- [27] Karamanis P.; Bégué D.; Pouchan C. *J. Chem. Phys.* **2007**, 127, 094706.
- [28] Karamanis P.; Pouchan C.; Weatherford C. A.; Gutsev G. L. *J. Phys. Chem. C* **2011**, 115, 97–107.
- [29] Brédas J. L.; Adant C.; Tackx P.; Persoons A.; Pierce B. M. *Chem. Rev.* **1994**, 94, 243–278.
- [30] Wang J.; Zhu L.; Zhang X.; Yang M. *J. Phys. Chem. A* **2008**, 112, 8226–8230.
- [31] Xu H.; Li Z.; Wang F.; Wu D.; Harigaya K.; Gu F. *Chem. Phys. Lett.* **2008**, 454, 323–326.
- [32] Pradhan P.; Ray A. K. *J. Mol. Struct. (THEOCHEM)* **2005**, 716, 109–130.
- [33] Deng J. L.; Su K. H.; Wang X.; Zeng Q. F.; Cheng L. F.; Xu Y. D.; Zhang L. T. *Eur. Phys. J. D* **2008**, 49, 21–35.
- [34] Duan X. F.; Wei J.; Burggraf L.; Weeks D. *Comp. Mater. Sci.* **2010**, 47, 630–644.
- [35] Froudakis G.; Zdetsis A.; Mühlhäuser M.; Engels B.; Peyerimhoff S. D. *J. Chem. Phys.* **1994**, 101, 6790–6799.
- [36] Alberts I. L.; Grev R. S.; Schaefer III H. F. *J. Chem. Phys.* **1990**, 93, 5046–5052.
- [37] McCarthy M. C.; Apponi A. J.; Thaddeus P. *J. Chem. Phys.* **1999**, 110, 10645–10648.
- [38] McCarthy M. C.; Apponi A. J.; Thaddeus P. *J. Chem. Phys.* **1999**, 111, 7175–7178.
- [39] Rintelman J. M.; Gordon M. S. *J. Chem. Phys.* **2001**, 115, 1795–1803.
- [40] Sattelmeyer K. W.; Schaefer III H. F. *J. Chem. Phys.* **2002**, 116, 9151–9153.
- [41] Hirschfelder J. O.; Curtis C. F.; Bird R. B. *Molecular Theory of Gases and Liquids*, Wiley, New York, 1954, p950.
- [42] Maroulis G. *J. Phys. Chem.* **1996**, 100, 13466–13473.
- [43] Castro M. A.; Canuto S. *Phys. Rev. A* **1993**, 48, 826–828.
- [44] Frisch, M. J.; Trucks, G. W.; Schlegel, H. B.; Scuseria, G. E.; Robb, M. A.; Cheeseman, J. R.; Montgomery, Jr., J. A.; Vreven, T.; Kudin, K. N.; Burant, J. C.; Millam, J. M.; Iyengar, S. S.; Tomasi, J.; Barone, V.; Mennucci, B.; Cossi, M.; Scalmani, G.; Rega, N.; Petersson, G. A.; Nakatsuji, H.; Hada, M.; Ehara, M.; Toyota, K.; Fukuda, R.; Hasegawa, J.; Ishida, M.; Nakajima, T.; Honda, Y.; Kitao, O.; Nakai, H.; Klene, M.; Li, X.; Knox, J. E.; Hratchian, H. P.; Cross, J. B.; Bakken, V.; Adamo, C.; Jaramillo, J.; Gomperts, R.; Stratmann, R. E.; Yazyev, O.; Austin, A. J.; Cammi, R.; Pomelli, C.; Ochterski, J. W.; Ayala, P. Y.; Morokuma, K.; Voth, G. A.; Salvador, P.; Dannenberg, J. J.; Zakrzewski, V. G.; Dapprich, S.; Daniels, A. D.; Strain, M. C.; Farkas, O.; Malick, D. K.; Rabuck, A. D.; Raghavachari, K.; Foresman, J. B.; Ortiz, J. V.; Cui, Q.; Baboul, A. G.; Clifford, S.; Cioslowski, J.; Stefanov, B. B.; Liu, G.; Liashenko, A.; Piskorz, P.; Komaromi, I.; Martin, R. L.; Fox, D. J.; Keith, T.; Al-Laham, M. A.; Peng, C. Y.; Nanayakkara, A.; Challacombe, M.; Gill, P. M. W.; Johnson, B.; Chen, W.; Wong, M. W.; Gonzalez, C.; Pople, J. A. *Gaussian 03*, Revision D.01, Gaussian, Inc., Wallingford, CT, **2004**.
- [45] Fuentealba P. *Phys. Rev. A* **1998**, 58, 4232–4234.
- [46] Wang J. L.; Yang M. L.; Wang G. H.; Zhao J. J. *Chem. Phys. Lett.* **2003**, 367, 448–454.
- [47] Proft F. D.; Sablon N.; Tozer D. J.; Geerlings P. *Faraday Discuss.* **2007**, 135, 151–159.
- [48] Nalwa H.S., *Handbook of Thin Films Materials*, Volume 5: Nanomaterials and Magnetic Thin Films. Academic Press, New York, and 2002, Chapter 2
- [49] Chattaraj P. K.; Sengupta S. *J. Phys. Chem.* **1996**, 100, 16126–16130.
- [50] Hohm U. *J. Phys. Chem. A* **2000**, 104, 8418–8423.
- [51] Parr R. G.; Chattaraj P. K. *J. Am. Chem. Soc.* **1991**, 113, 1854–1855.

- [52] Kanis D. R.; Ratner M. A.; Marks T. J. *Chem. Rev.* **1994**, 94, 195–242.
 [53] Brédas J. L. *Science* **1994**, 263, 487–488.
 [54] Hunsicker S.; Jones R. O. *J. Chem. Phys.* **1996**, 105, 5048–5060.
 [55] Gomei M.; Kishi R.; Nakajima A.; Iwata S.; Kaya K. *J. Chem. Phys.* **1997**, 107, 10051–10061.
 [56] Bertolus M.; Brenner V.; Millié P. *Eur. Phys. J. D* **1998**, 1, 197–205.
 [57] Jiang Z. Y.; Xu X. H.; Wu H. S.; Jin Z. H. *J. Phys. Chem. A* **2003**, 107, 10126–10131.
 [58] Huda M. N.; Ray A. K. *Phys. Rev. A* **2004**, 69, 011201.
 [59] Hou J. Y.; Song B. *J. Chem. Phys.* **2008**, 128, 154304.
 [60] Grozema F. C.; Telesca R.; Jonkman H. T.; Siebbeles L. D. A.; Snijders J. G. *J. Chem. Phys.* **2001**, 115, 10014.
 [61] Ruud K.; Mennucci B.; Cammi R.; Frediani L. *J. Comp. Meth. Sci. Eng.* **2004**, 4, 381–397

Table 1. Δq_x , α_{xx} , Δq_y , α_{yy} , Δq_z , α_{zz} , and Δq of Si_mC_n ($m, n = 1 - 4$) clusters. "L", "P", and "C" indicate the linear, prolate, and compact clusters, respectively.

Cluster	Δq_x (e)	α_{xx} (\AA^3)	Δq_y (e)	α_{yy} (\AA^3)	Δq_z (e)	α_{zz} (\AA^3)	Δq (e/atom)
SiC (L, $C_{\infty v}$) ^a	0.017	8.48	0.017	8.48	0.563	8.82	0.100
SiC ₂ (P, C_{2v})	0.017	5.49	0.286	6.87	0.452	7.90	0.084
SiC ₂ (L, $C_{\infty v}$)	0.003	6.23	0.003	6.23	0.545	12.14	0.061
SiC ₃ (P, C_{2v}) (a)	0.013	6.47	0.367	7.39	0.441	10.55	0.068
SiC ₃ (P, C_{2v}) (b)	0.009	6.53	0.238	9.56	0.466	9.15	0.059
SiC ₃ (L, $C_{\infty v}$)	0.013	7.21	0.013	7.21	0.932	21.95	0.080
SiC ₄ (P, C_{2v})	0.005	6.72	0.542	13.20	0.359	9.34	0.060
SiC ₄ (L, $C_{\infty v}$)	0.011	7.79	0.011	7.79	0.895	29.69	0.061
Si ₂ C (P, C_{2v})	0.000	9.02	0.709	18.24	0.263	9.05	0.108
Si ₂ C (L, $D_{\infty h}$)	0.003	9.26	0.003	9.27	0.722	19.10	0.081
Si ₂ C ₂ (P, D_{2h})	0.011	8.55	0.244	9.09	0.597	16.57	0.071
Si ₂ C ₂ (L, $D_{\infty h}$)	0.023	10.13	0.023	10.13	1.330	36.69	0.115
Si ₂ C ₃ (P, C_{2v})	0.009	9.78	0.925	25.43	0.467	10.53	0.093
Si ₂ C ₃ (L, $D_{\infty h}$)	0.011	10.59	0.011	10.59	1.201	42.65	0.082
Si ₂ C ₄ (L, $D_{\infty h}$)	0.006	11.73	0.006	11.73	1.641	67.88	0.092
Si ₂ C ₄ (P, C_s)	0.422	12.08	0.755	19.25	0.319	13.74	0.083
Si ₃ C (P, C_{2v})	0.002	11.06	0.761	21.66	0.677	15.27	0.120
Si ₃ C (P, C_s)	0.276	11.95	0.789	17.59	0.719	20.52	0.149
Si ₃ C ₂ (P, C_{2v}) (a)	0.036	12.12	1.267	31.64	0.417	13.96	0.115
Si ₃ C ₂ (C, C_{2v}) (b)	0.371	14.07	0.618	19.27	0.851	17.98	0.123
Si ₃ C ₃ (P, C_s) (a)	0.192	15.52	0.842	13.10	0.641	21.09	0.093
Si ₃ C ₃ (C, C_s) (b)	0.636	12.78	0.470	20.76	0.692	22.96	0.100
Si ₃ C ₄ (P, C_{2v}) (a)	0.008	21.21	0.874	13.63	0.706	26.50	0.076
Si ₃ C ₄ (C, C_{2v}) (b)	0.714	32.91	0.317	19.52	0.989	13.07	0.096
Si ₃ C ₄ (P, C_s)	0.992	12.63	0.758	28.17	0.050	21.04	0.086

Si ₄ C (C, C _{2v})	0.813	23.56	0.621	21.35	0.715	18.02	0.143
Si ₄ C (C, C _{3v})	0.923	21.61	0.880	21.61	0.707	18.43	0.167
Si ₄ C ₂ (C, C _{2v})	0.650	20.23	0.803	26.42	0.417	15.17	0.104
Si ₄ C ₂ (C, D _{2d})	0.714	22.21	0.714	22.21	0.438	14.47	0.104
Si ₄ C ₃ (P, C ₁)	1.184	33.66	1.010	26.44	0.466	16.57	0.127
Si ₄ C ₃ (P, C _s)	0.929	26.12	1.292	35.21	0.466	15.16	0.128
Si ₄ C ₄ (P, C _{2v})	0.023	15.85	1.298	34.49	1.683	32.76	0.125
Si ₄ C ₄ (P, C _s) (a)	0.924	28.70	1.310	35.99	0.026	15.95	0.094
Si ₄ C ₄ (C, C _s) (b)	0.430	18.48	0.706	25.80	0.699	26.27	0.076
Si ₄ C ₄ (C, C _s) (c)	0.722	22.18	0.924	30.16	0.574	22.49	0.092

^a cluster shape and symmetry.

List of figure captions:

Figure 1. Geometries of Si_mC_n ($m, n = 1 - 4$) clusters. "L", "P", and "C" indicate the linear, prolate, and compact clusters, respectively. ^a Electronic state and symmetry. ^b Binding energy (in eV/atom) and energy gap (in eV). ^c Cluster shape and $\langle\alpha\rangle$ (in Å³/atom).

Figure 2. Polarizabilities versus the cluster size (N) for Si_mC_n ($m, n = 1 - 4$), Si_m ($m = 1 - 8$), and C_n (linear: $n = 1 - 8$, cyclic: $n = 4, 6$, and 8) clusters. The polarizabilities of cyclic C_n ($n = 4, 6$, and 8) clusters are 1.39, 1.44, and 1.50 Å³/atom, respectively. Dot line: Si bulk, Solid line: SiC bulk, Dash line: C bulk.

Figure 3. Polarizabilities versus the E_g values for Si_mC_n ($m, n = 1 - 4$) clusters.

Figure 4. Polarizabilities versus the E_b values for Si_mC_n ($m, n = 1 - 4$) clusters. The dot line indicates an approximate linear correlation between α and E_b .

Figure 5. Polarizabilities versus the Δq values for Si_mC_n ($m, n = 1 - 4$) clusters. The dot line indicates an approximate linear correlation between α and Δq .

Figure 6. Shape dependence of the $\langle\alpha\rangle$ values for Si_mC_n ($m, n = 1 - 4$) clusters.

Figure 7. (a) Polarizabilities, (b) Binding energies, (c) Energy gaps, and (d) Δq versus the number of C atoms (n) in cluster with both the cluster shape and the number of Si atoms fixed. (L), (P), and (C) indicate the linear, prolate, and compact clusters, respectively. (+3.0) indicates 3.0 is added to the $\langle\alpha\rangle$ values to clearly display the plots. Other factors have a similar meaning.

Figure 8. HOMO-1, HOMO, LUMO, and LUMO+1 of SiC₂, SiC₄, Si₃C₂, Si₃C₃, and Si₄C₄ clusters.

Figure 9. Polarizabilities versus the cluster composition (*i.e.*, m/n ratio) for Si_mC_n ($m, n = 1 - 4$) clusters.

Figure 10. Polarizabilities ($\text{\AA}^3/\text{atom}$), E_b (eV/atom), E_g (eV), and Δq (e/atom) versus the number of Si atoms (m) in cluster with the number of C atoms fixed. (+1.0) indicates 1.0 is added to the E_b values to clearly display the plots. Other factors have a similar meaning.

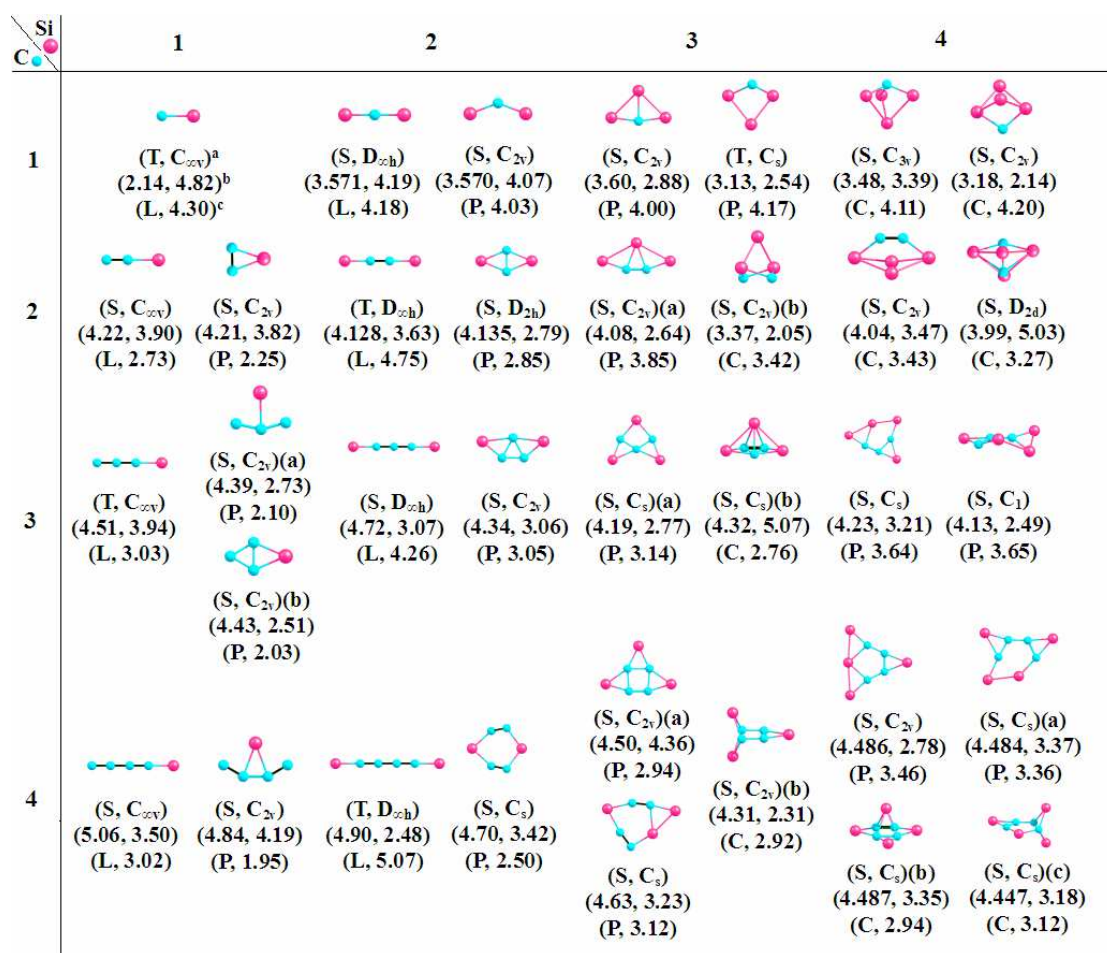


Figure 1. Geometries of Si_mC_n ($m, n = 1 - 4$) clusters. "L", "P", and "C" indicate the linear, prolate, and compact clusters, respectively.

^a Electronic state and symmetry.

^b Binding energy (in eV/atom) and energy gap (in eV).

^c Cluster shape and $\langle \alpha \rangle$ (in $\text{\AA}^3/\text{atom}$).

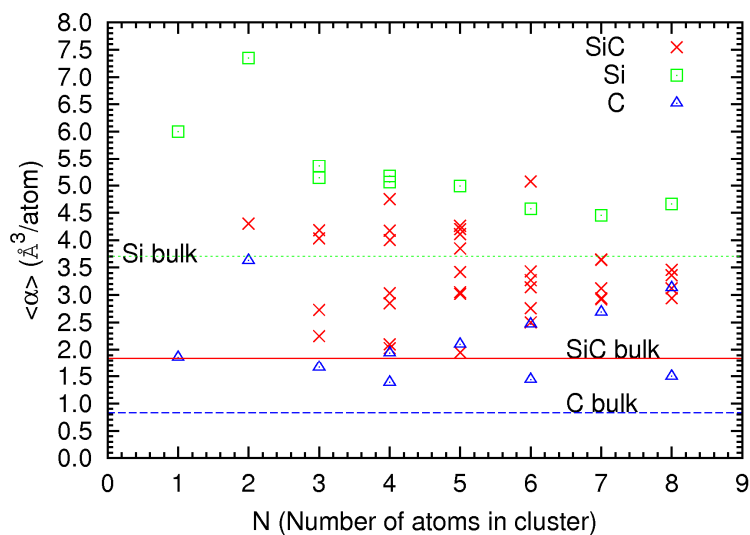


Figure 2. Polarizabilities versus the cluster size (N) for Si_mC_n ($m, n = 1 - 4$), Si_m ($m = 1 - 8$), and C_n (linear: $n = 1 - 8$, cyclic: $n = 4, 6$, and 8) clusters. The polarizabilities of cyclic C_n ($n = 4, 6$, and 8) clusters are $1.39, 1.44$, and $1.50 \text{ \AA}^3/\text{atom}$, respectively. Dot line: Si bulk, Solid line: SiC bulk, Dash line: C bulk.

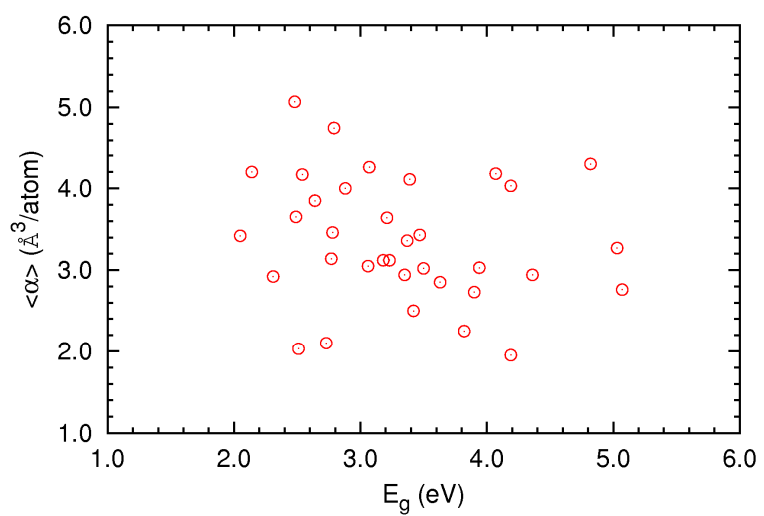


Figure 3. Polarizabilities versus the E_g values for Si_mC_n ($m, n = 1 - 4$) clusters.

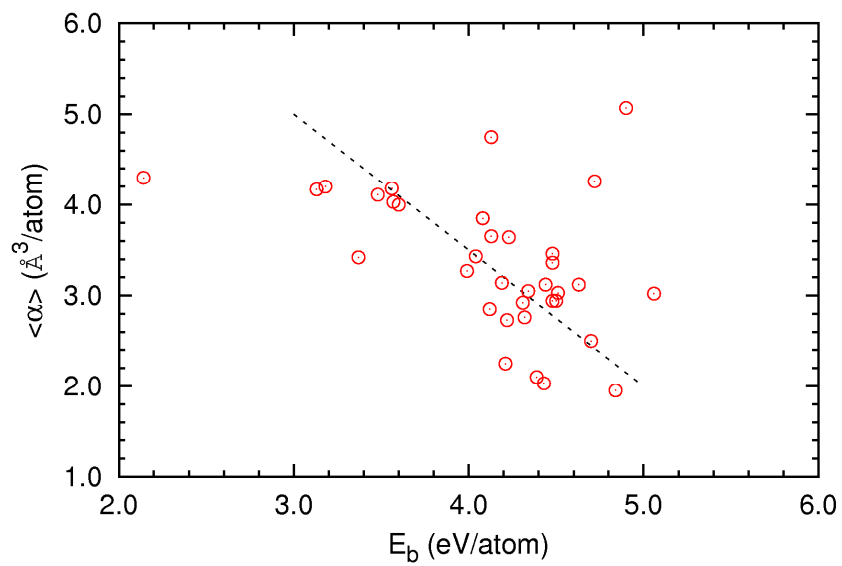


Figure 4. Polarizabilities versus the E_b values for Si_mC_n ($m, n = 1 - 4$) clusters. The dot line indicates an approximate linear correlation between α and E_b .

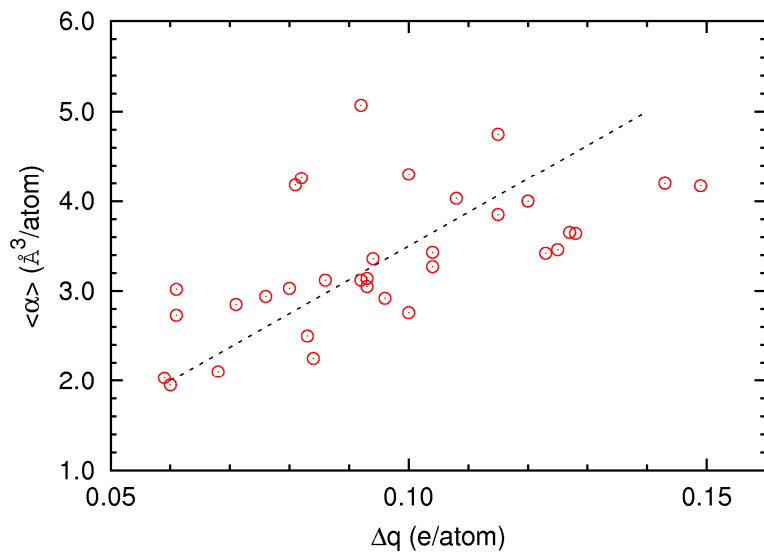


Figure 5. Polarizabilities versus the Δq values for Si_mC_n ($m, n = 1 - 4$) clusters. The dot line indicates an approximate linear correlation between α and Δq .

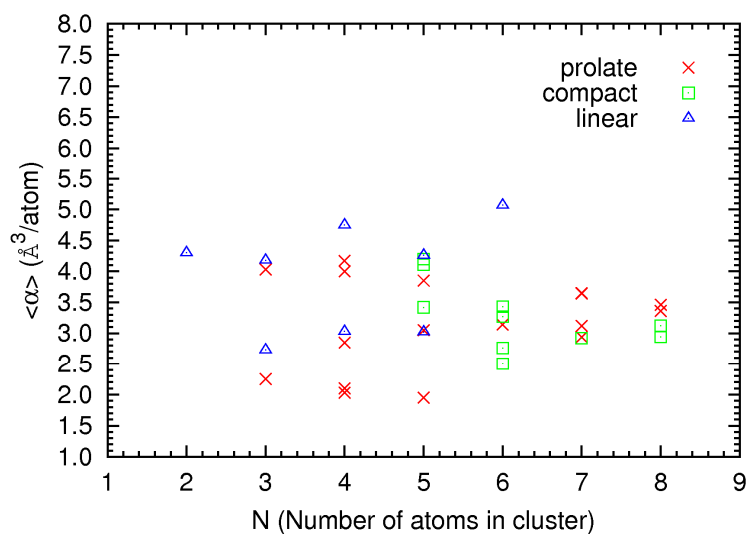
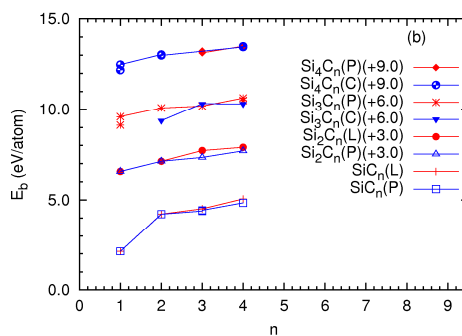
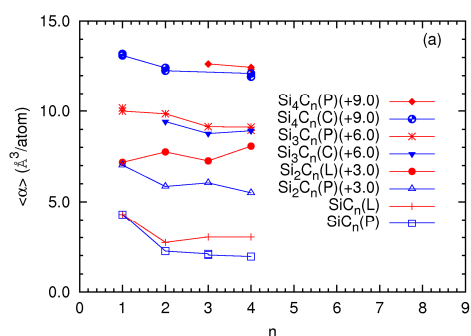


Figure 6. Shape dependence of the $\langle \alpha \rangle$ values for Si_mC_n ($m, n = 1 - 4$) clusters.



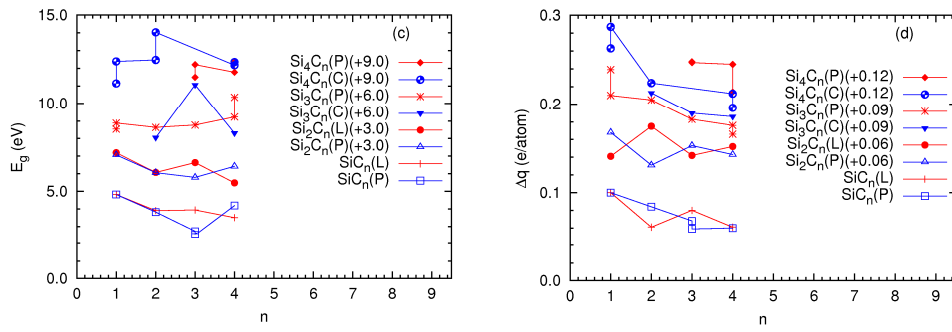


Figure 7. (a) Polarizabilities, (b) Binding energies, (c) Energy gaps, and (d) Δq versus the number of C atoms (n) in cluster with both the cluster shape and the number of Si atoms fixed. (L), (P), and (C) indicate the linear, prolate, and compact clusters, respectively. (+3.0) indicates 3.0 is added to the $\langle \alpha \rangle$ values to clearly display the plots. Other factors have a similar meaning.

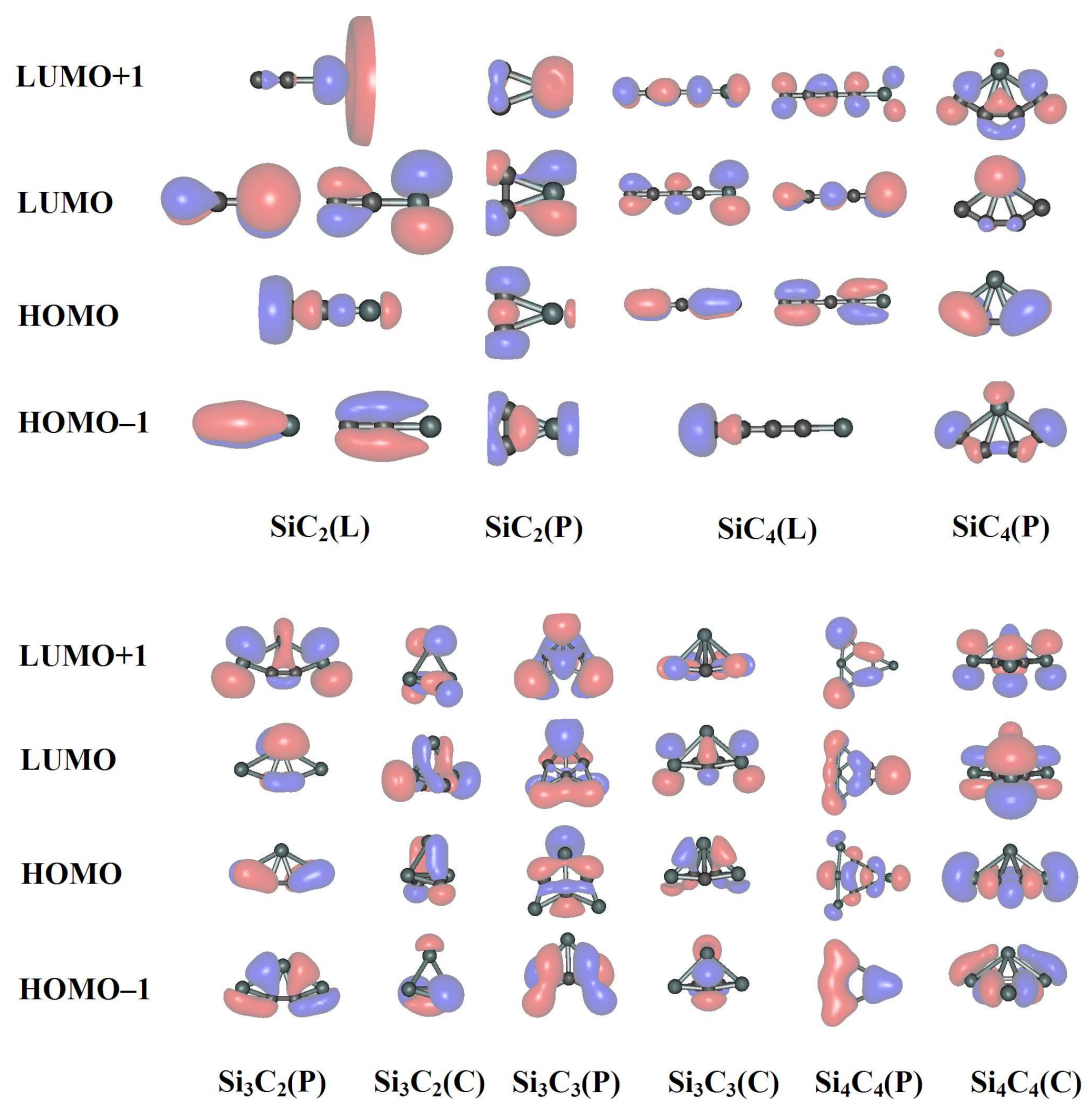


Figure 8. HOMO-1, HOMO, LUMO, and LUMO+1 of SiC₂, SiC₄, Si₃C₂, Si₃C₃, and Si₄C₄ clusters.

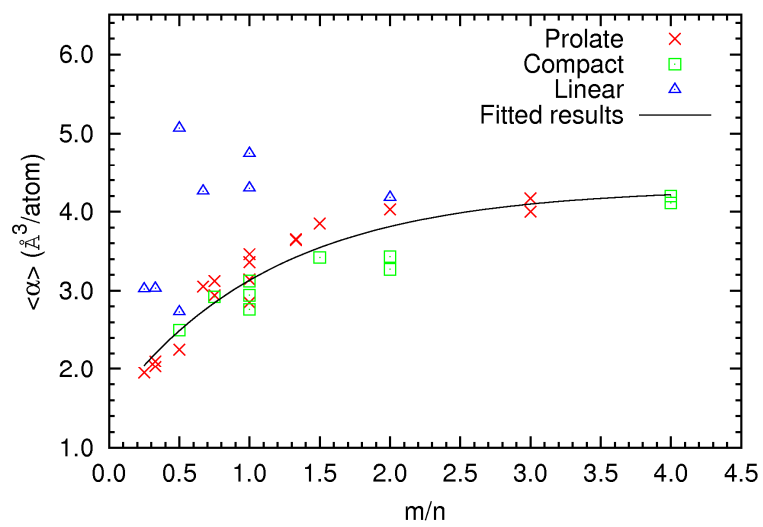


Figure 9. Polarizabilities versus the cluster composition (*i.e.*, m/n ratio) for Si_mC_n ($m, n = 1 - 4$) clusters.

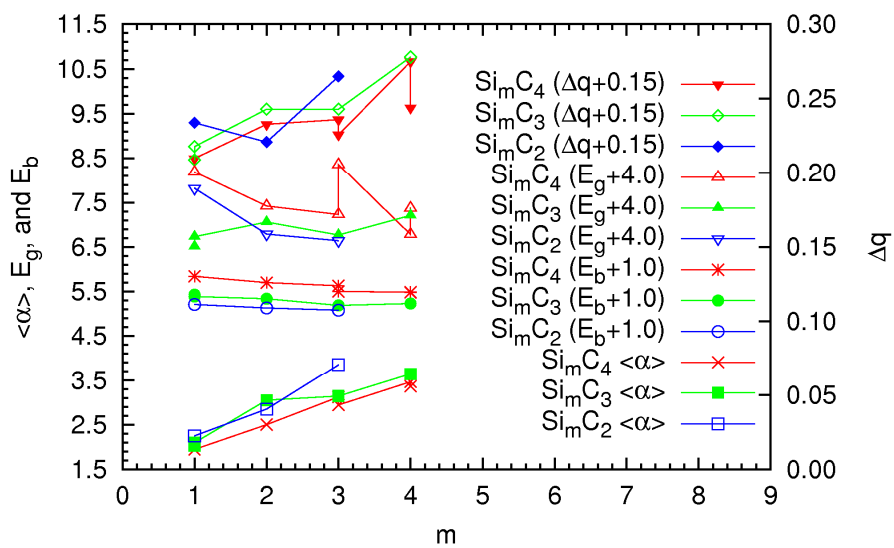


Figure 10. Polarizabilities ($\text{\AA}^3/\text{atom}$), E_b (eV/atom), E_g (eV), and Δq (e/atom) versus the number of Si atoms (m) in cluster with the number of C atoms fixed. (+1.0) indicates 1.0 is added to the E_b values to clearly display the plots. Other factors have a similar meaning.